Global Network Reorganization During Dynamic Adaptations of Bacillus subtilis Metabolism

Joerg Martin Buescher, Wolfram Liebermeister, Matthieu Jules, Markus Uhr, Jan Muntel, Eric Botella, Bernd Hessling, Roelco Jacobus Kleijn, Ludovic Le Chat, François Lecointe, et al.

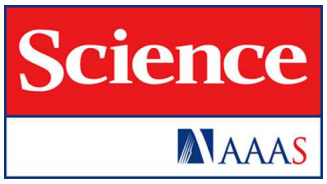

Global Network Reorganization During Dynamic Adaptations of *Bacillus subtilis* Metabolism

Joerg Martin Buescher *et al.*

Science **335**, 1099 (2012);
DOI: 10.1126/science.1206871

Science (print ISSN 0036-8075; online ISSN 1095-9203) is published weekly, except the last week in December, by the American Association for the Advancement of Science, 1200 New York Avenue NW, Washington, DC 20005.

loosening needed for growth. Increased wall remodeling is expected to change elastic properties, which explains why fast-growing areas in the peripheral region can stay in their linear range of elasticity for larger deformations (*20*–*22*); while at the same time, they are stiffer than slow-growing regions for small strains. Our data suggest that the functional distinction between slow- and fast-growing regions in the shoot apex is not only genetically defined (*30*, *31*) but is enhanced by mechanical feedbacks. Such a mechanism would stabilize and protect the critically important stem cell niche from the numerous sources of noise inherent in the chemistry of biological systems.

References and Notes

1. T. Steeves, I. Sussex, Eds., *Patterns in Plant Development* (Cambrige Univ. Press, New York, 1988).
2. D. Kwiatkowska, J. Dumais, *J. Exp. Bot.* **54**, 1585 (2003).
3. O. Grandjean *et al*., *Plant Cell* **16**, 74 (2004).
4. G. V. Reddy, M. G. Heisler, D. W. Ehrhardt, E. M. Meyerowitz, *Development* **131**, 4225 (2004).
5. S. Vanneste, J. Friml, *Cell* **136**, 1005 (2009).
6. M. G. Heisler *et al*., *Curr. Biol.* **15**, 1899 (2005).
7. D. Reinhardt *et al*., *Nature* **426**, 255 (2003).
8. D. L. Rayle, R. E. Cleland, *Plant Physiol.* **99**, 1271 (1992).
9. D. J. Cosgrove, *Nat. Rev. Mol. Cell Biol.* **6**, 850 (2005).
10. T. Vernoux, J. Kronenberger, O. Grandjean, P. Laufs, J. Traas, *Development* **127**, 5157 (2000).
11. D. Reinhardt, T. Mandel, C. Kuhlemeier, *Plant Cell* **12**, 507 (2000).
12. A. Fleming, S. McQueen-Mason, T. Mandel, C. Kuhlemeier, *Science* **276**, 1415 (1997).
13. S. Pien, J. Wyrzykowska, S. McQueen-Mason, C. Smart, A. Fleming, *Proc. Natl. Acad. Sci. U.S.A.* **98**, 11812 (2001).
14. A. Peaucelle *et al*., *Curr. Biol.* **18**, 1943 (2008).
15. A. Peaucelle *et al*., *Curr. Biol.* **21**, 1720 (2011).
16. M. G. Heisler *et al*., *PLoS Biol.* **8**, e1000516 (2010).
17. O. Hamant *et al*., *Science* **322**, 1650 (2008).
18. P. Milani *et al*., *Plant J.* **67**, 1116 (2011).
19. Materials and methods are available as supporting material on *Science* Online
20. C. Storm, J. J. Pastore, F. C. MacKintosh, T. C. Lubensky, P. A. Janmey, *Nature* **435**, 191 (2005).
21. S. E. Whitney, M. G. Gothard, J. T. Mitchell, M. J. Gidley, *Plant Physiol.* **121**, 657 (1999).
22. R. R. Vincent, D. N. Pinder, Y. Hemar, M. A. Williams, *Phys. Rev. E Stat. Nonlin. Soft Matter Phys.* **76**, 031909 (2007).
23. J. Dumais, C. R. Steele, *J. Plant Growth Regul.* **19**, 7 (2000).
24. J. M. Selker, G. L. Steucek, P. B. Green, *Dev. Biol.* **153**, 29 (1992).
25. R. Vandiver, A. Goriely, *Philos. Transact. A Math. Phys. Eng. Sci.* **367**, 3607 (2009).
26. V. Mirabet, P. Das, A. Boudaoud, O. Hamant, *Annu. Rev. Plant Biol.* **62**, 365 (2011).
27. U. Kutschera, K. J. Niklas, *J. Plant Physiol.* **164**, 1395 (2007).
28. J. A. Lockhart, *J. Theor. Biol.* **8**, 264 (1965).
29. T. Vernoux *et al*., *Mol. Syst. Biol.* **7**, 508 (2011).
30. R. Sablowski, *Curr. Opin. Plant Biol.* **10**, 639 (2007).
31. R. K. Yadav, T. Girke, S. Pasala, M. Xie, G. V. Reddy, *Proc. Natl. Acad. Sci. U.S.A.* **106**, 4941 (2009).

Acknowledgments: We thank J. Dumais, A. Fleming, S. Robinson, D. Kwiatkowska, and P. Wojtaszek for reading the manuscript. This work was supported by the Swiss National Science Foundation, SystemsX.ch, and the European Union New and Emerging Science and Technology grant MechPlant. N.N. received European Molecular Biology Organization Long-Term and Roche Research Foundation fellowships.

Supporting Online Material

www.sciencemag.org/cgi/content/full/335/6072/1096/DC1
Materials and Methods
Figs. S1 to S8
References (*32*–*41*)

24 August 2011; accepted 30 January 2012
10.1126/science.1213100

Global Network Reorganization During Dynamic Adaptations of *Bacillus subtilis* Metabolism

Joerg Martin Buescher,[1]* Wolfram Liebermeister,[2]* Matthieu Jules,[3]* Markus Uhr,[4]* Jan Muntel,[5]* Eric Botella,[7] Bernd Hessling,[5] Roelco Jacobus Kleijn,[1] Ludovic Le Chat,[3] François Lecointe,[3] Ulrike Mäder,[5] Pierre Nicolas,[6] Sjouke Piersma,[8] Frank Rügheimer,[15] Dörte Becher,[5] Philippe Bessieres,[6] Elena Bidnenko,[3] Emma L. Denham,[8] Etienne Dervyn,[3] Kevin M. Devine,[7] Geoff Doherty,[9] Samuel Drulhe,[15] Liza Felicori,[10] Mark J. Fogg,[11] Anne Goelzer,[6] Annette Hansen,[7] Colin R. Harwood,[12] Michael Hecker,[5] Sebastian Hubner,[7] Claus Hultschig,[13] Hanne Jarmer,[14] Edda Klipp,[2] Aurélie Leduc,[6] Peter Lewis,[9] Frank Molina,[10] Philippe Noirot,[3] Sabine Peres,[10] Nathalie Pigeonneau,[3] Susanne Pohl,[12] Simon Rasmussen,[14] Bernd Rinn,[13] Marc Schaffer,[5] Julian Schnidder,[1] Benno Schwikowski,[15] Jan Maarten Van Dijl,[8] Patrick Veiga,[6] Sean Walsh,[13] Anthony J. Wilkinson,[11] Jörg Stelling,[4]† Stéphane Aymerich,[3]† Uwe Sauer[1]†

Adaptation of cells to environmental changes requires dynamic interactions between metabolic and regulatory networks, but studies typically address only one or a few layers of regulation. For nutritional shifts between two preferred carbon sources of *Bacillus subtilis*, we combined statistical and model-based data analyses of dynamic transcript, protein, and metabolite abundances and promoter activities. Adaptation to malate was rapid and primarily controlled posttranscriptionally compared with the slow, mainly transcriptionally controlled adaptation to glucose that entailed nearly half of the known transcription regulation network. Interactions across multiple levels of regulation were involved in adaptive changes that could also be achieved by controlling single genes. Our analysis suggests that global trade-offs and evolutionary constraints provide incentives to favor complex control programs.

A major challenge in biology is to understand the organization and interactions of the various functional and regulatory networks in cells. The underlying complexity arises from the intertwined nonlinear and dynamic interactions among a large number of cellular components. To better understand these interacting molecular networks, the acquisition of appropriate, preferably time-resolved quantitative data is a prerequisite (*1*–*3*). Because the acquisition of such data is technically demanding, few studies have reported transcript, protein, and metabolite abundances, and most studies have been restricted to steady-state conditions (*4*–*8*). Consequently, only subsets of components have been monitored dynamically for very short- (*9*, *10*) or long-term responses (*11*, *12*) to environmental perturbations. These studies typically revealed coordinated abundance changes (*11*, *12*), major transcriptional reconfigurations in response to environmental change (*9*, *11*), and an unanticipated complexity of unicellular organisms (*7*). Data interpretation, however, has generally been restricted to multivariate statistical analysis methods that indicate general but not mechanistic relationships between different molecular entities. Focusing on single data types with sophisticated computational analysis has been informative (*3*) but increases the risk of missing the functionally relevant multilevel control mechanisms (*2*), limiting the description of the underlying molecular mechanisms and, hence, the depth of biological insight.

[1]Institute of Molecular Systems Biology, ETH Zurich, 8093 Zurich, Switzerland. [2]Theoretical Biophysics, Humboldt University Berlin, 10115 Berlin, Germany. [3]INRA, UMR1319 Micalis, Jouy-en-Josas F78350, France. [4]Department of Biosystems Science and Engineering, ETH Zurich, 4058 Basel, Switzerland. [5]Institute for Microbiology, Ernst-Moritz-Arndt-University Greifswald, 17487 Greifswald, Germany. [6]INRA, Mathématique Informatique et Génome UR1077, 78350 Jouy-en-Josas, France. [7]Smurfit Institute of Genetics, Trinity College Dublin, Dublin 2, Ireland. [8]Department of Medical Microbiology, University of Groningen and University Medical Center Groningen, 9700 RB Groningen, Netherlands. [9]School of Environmental and Life Sciences, University of Newcastle, Callaghan, NSW 2308, Australia. [10]Sysdiag CNRS Bio-Rad UMR 3145, Cap Delta/Parc Euromédecine, 34184 Montpellier Cedex 4, France. [11]York Structural Biology Laboratory, Department of Chemistry, University of York, York YO10 5YW, UK. [12]Institute, of Cell and Molecular Biosciences, Centre for Bacterial Cell Biology, University of Newcastle upon Tyne, Newcastle upon Tyne, NE2 4AX, UK. [13]Center for Information Sciences and Databases, Department of Biosystems Science and Engineering, ETH Zurich, 4058 Basel, Switzerland. [14]Center for Biological Sequence Analysis, Department of Systems Biology, Technical University of Denmark, 2800 Kgs. Lyngby, Denmark. [15]Institut Pasteur, Systems Biology Lab, Department of Genomes and Genetics, and CNRS URA 2171, F-75015 Paris, France.

*These authors contributed equally to this work.
†To whom correspondence should be addressed. E-mail: joerg.stelling@bsse.ethz.ch (J.S.); stephane.aymerich@grignon.inra.fr (S.A.); sauer@ethz.ch (U.S.)

To elucidate the dynamic interplay between metabolic and regulatory networks systematically, we investigated dynamic shifts in availability of the preferred carbon sources, glucose and malate, of the bacterium *Bacillus subtilis* (*13*). Because these nutrients repress the use of other substrates but are themselves used together, they represent a tractable model for analyzing dynamic decision-making by cells when faced with compounds of similar nutritional value. We induced dynamic shifts by adding glucose or malate to cultures of *B. subtilis* growing exponentially on the other substrate. To elucidate the cellular adaptation mechanisms, we determined transcript, protein, and absolute metabolite abundances, as well as promoter activities (Fig. 1 and table S1) (*14*), providing dynamic data with up to 24 time points for two shift experiments that cover short-term metabolic to longer-term protein-level adaptation (*15*).

To enable data integration, we developed problem-driven, yet generic solutions in three areas (table S1). To generate consistent data, we minimized biological variability (Fig. 1) by withdrawing samples from the same bioreactor culture in triplicate experiments (fig. S1) and, in a few cases, from standardized small-scale cultivations (fig. S2). We used naming and formatting conventions with unique identifiers for all considered constituents to permit the efficient exchange of data and knowledge. Furthermore, to maximize reliability and coverage for subsequent data analysis and modeling, we combined overlapping dynamic data acquired from different analytical platforms and on different time scales (Fig. 1). Data from the different transcript-array platforms did not require further consolidation (figs. S3 and S4), but we generated consensus proteomics data by calculating confidence-weighted averages of protein abundances obtained from two-dimensional gels and liquid chromatography–mass spectrometry (SOM 1). Replicate time series of transcript and protein data were then smoothed and interpolated by Bayesian multicurve regression analysis (SOM 1). Because metabolite data showed changes on various time scales, we developed a special algorithm that aligns time courses on the basis of Kalman smoothing (Fig. 2A and SOM 1) (*16*).

We exploited the profusion of data (table S1) to extend the genome annotation of *B. subtilis* by statistical data analysis and integration with prior knowledge (table S2). Analysis of mRNA

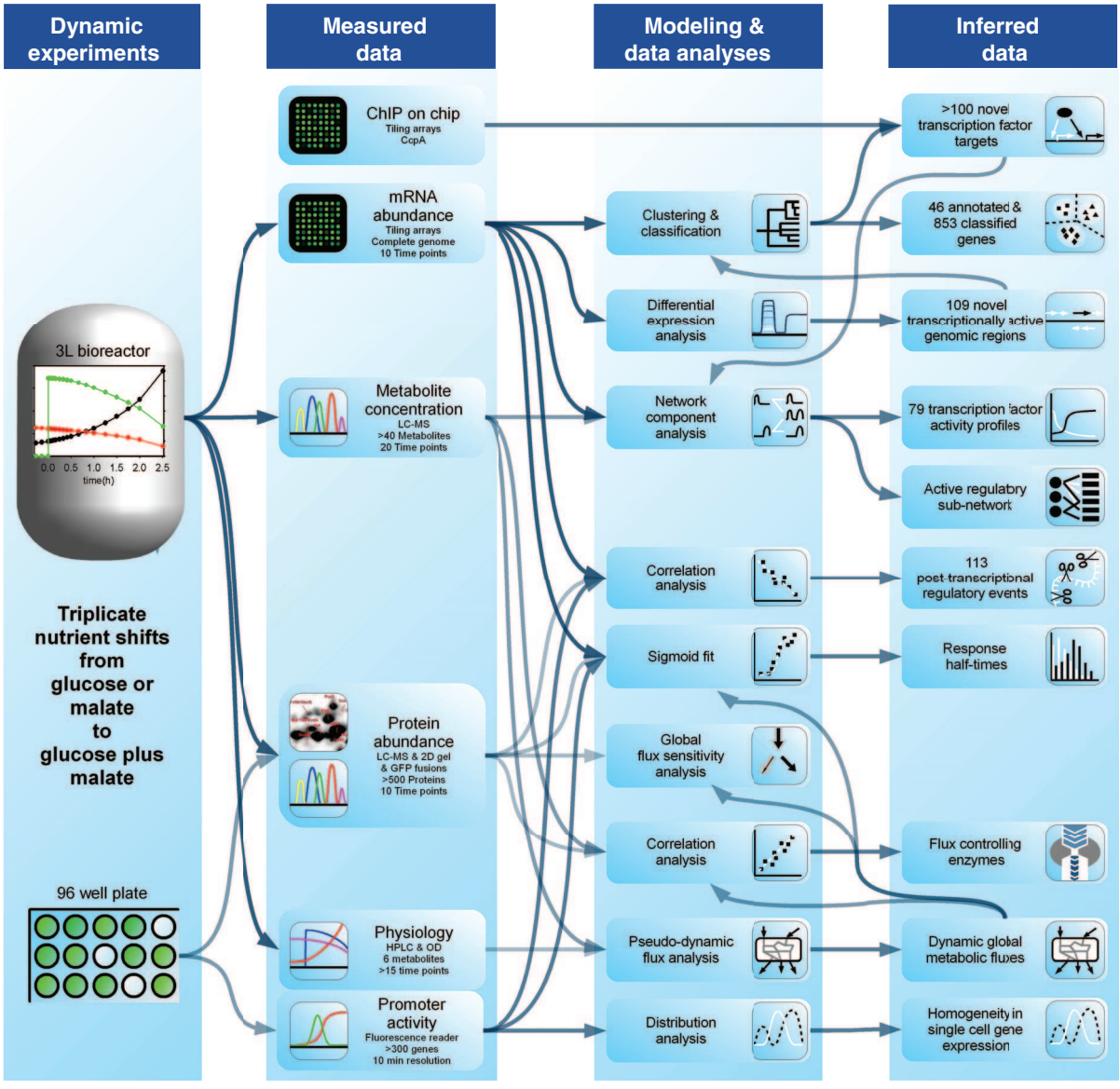

Fig. 1. Overview of our experimental design, computational analysis, and information flow. The dynamic shift experiments yielded measured data from which nonmeasurable quantities were inferred by statistical and model-based analysis. Arrows show the flow of information, including the use of inferred data as parameters for subsequent modeling steps. ChIP, chromatin immunoprecipitation; LC-MS, liquid chromatography–mass spectrometry; GFP, green fluorescent protein; HPLC, high-performance liquid chromatography; OD, optical density.

abundances identified 4393 transcriptionally active genomic regions, 109 of which were not previously described, including 21 putative protein-coding sequences and 23 antisense RNAs (table S3). Additionally, 2422 genomic regions were differentially transcribed after the nutrient shifts (table S1). Clustering of mRNA profiles and functional classification of differentially transcribed genes enabled detailed functional annotation of 46 genes (table S4) and probable function assignment of 853 previously not annotated genes (table S1). For the metabolically important transcription factors CcpA, CcpC, CcpN, and CggR (*17*–*19*), we identified DNA binding sites by chromatin immunoprecipitation–on-chip analysis in malate plus glucose (table S1). We found 184 CcpA binding sites, most of which were located near to promoters of genes differentially expressed immediately after glucose addition (fig. S5). By filtering this group for high-scoring, previously undetected CcpA sites, we generated an improved regulatory network topology (SOM 2) for subsequent analysis of regulatory events.

Metabolomics data revealed instantaneous malate uptake into cells grown on glucose but substantially delayed uptake of glucose into cells grown on malate (Fig. 2, B and C). Sensitivity analysis of steady-state fluxes in the stoichiometric network model in combination with proteomic data predicted transcriptional regulation to be more important for the dynamics induced by glucose than by malate (Fig. 2D). Network component analysis (*20*) quantified the strengths of all 2900 transcription factor interactions with target genes, and 1488 of the interactions were implicated in at least one shift (689 for malate addition; 1244 for glucose addition) (SOM 2). Furthermore, we identified 110 posttranscriptional regulation events in protein synthesis (77 and 23 were specific to malate and glucose addition, respectively) through a dynamic model that correlates time profiles of promoter activity, mRNA abundance, and protein abundance for 300 genes for which all three data types were available (tables S5 to S7). Overall, our integrated analysis suggests that apparently similar adaptation processes are mediated by fundamentally different control mechanisms, namely a predominantly posttranscriptional regulation after malate addition and a greater reliance on transcriptional regulation after glucose addition.

Next, we inferred the dynamic activity profiles of 154 transcription factors by network-component analysis (*20*) from the transcript abundances of

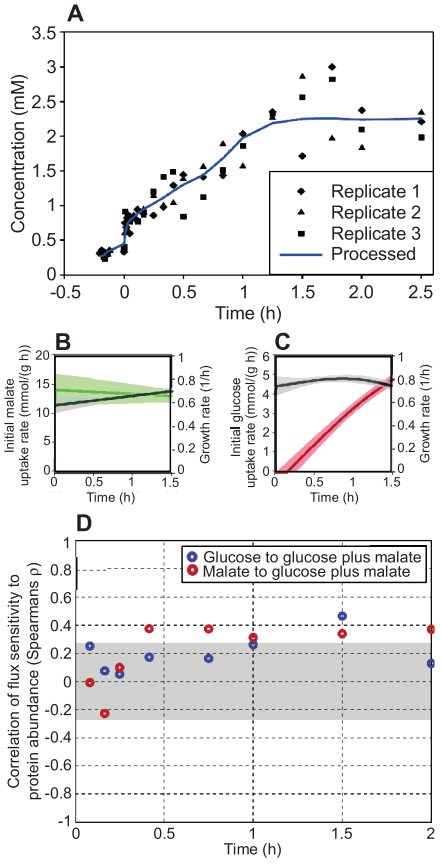

Fig. 2. (**A**) Processing of time-series data from parallel experiments. The example shown here is fructose 1,6-bisphosphate during the malate–to–glucose-plus-malate shift. Measurements from three independent cultures (black data points) yield an averaged and smooth time course (blue line). (**B** and **C**) Initial dynamic uptake rates of malate (green) and glucose (red) after addition to wild-type *B. subtilis* growing on the respective other substrate were obtained by fitting of splines. Black lines and shadings represent the specific growth rate and 95% confidence intervals, respectively (SOM 3). (**D**) The global importance of transcriptional regulation after glucose addition is confirmed by an increasing correlation (red) between flux sensitivity (measuring the impact of a change in environmental conditions on a metabolic flux) and protein abundance over time. This increase does not occur after malate addition (blue). White areas denote statistically significant correlation values with respect to an approximate 95% confidence interval; gray shaded areas denote the absence of statistically significant correlation.

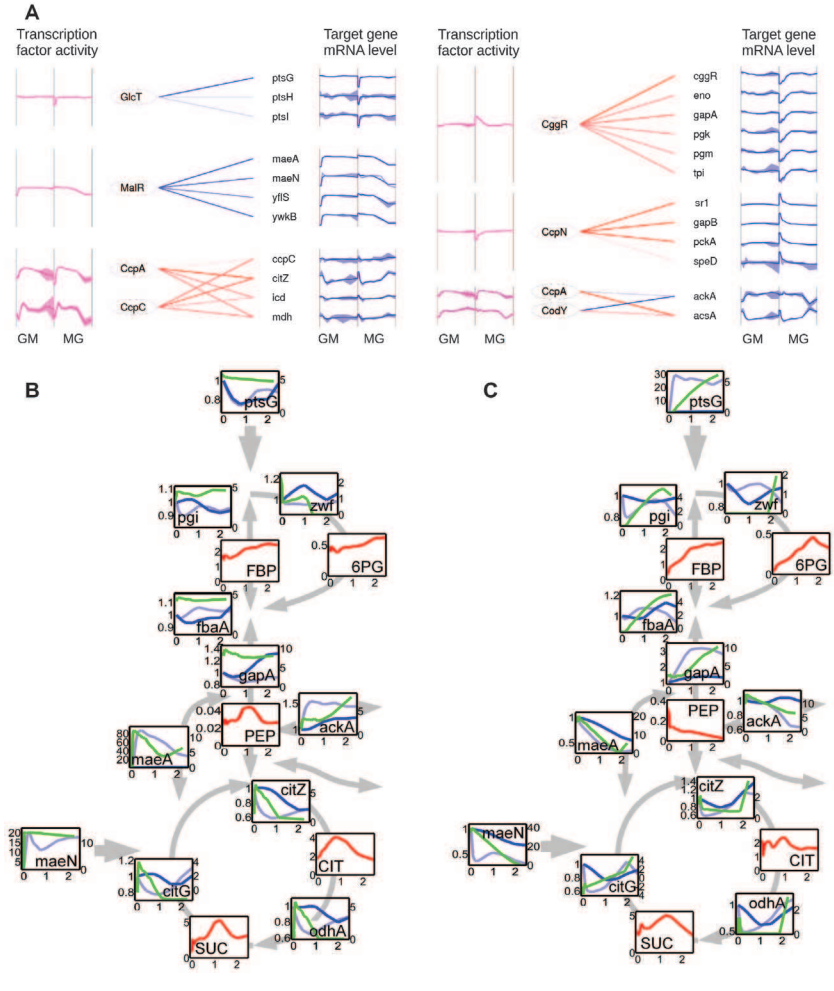

Fig. 3. (**A**) Activities of the main transcriptional regulators controlling central metabolism during the shifts of glucose (GM) or malate (MG) to glucose plus malate. Blue curves represent $\log_2$ expression profiles of target genes; purple curves denote the inferred transcription factor activities. Straight lines in the middle sections indicate the relative contribution (proportional to color intensity) of different transcription factors to target gene expression changes (blue, activation; red, repression). (**B** and **C**) Averaged time profiles of transcripts (light blue), proteins (dark blue), metabolic fluxes (green), and metabolites (red) during the dynamic shift experiments of glucose (B) or malate (C) to malate plus glucose.

their 1754 known target genes (Fig. 3A and SOM 2). One hundred twenty-seven transcription factors changed their activity profile significantly in at least one shift (61 for malate addition and 91 for glucose addition). A rapid change of activity (<5 min), most prominent for the transporter regulators MalR (malate) and GlcT (glucose), and the deviations between the inferred transcription factor activities and the measured transcription factor mRNA abundance provided evidence for posttranslational regulation (SOM 2). Network component analysis predicted that the activity of 51 transcription factors was modulated post-transcriptionally, and 39 of these (for example, NadR, KipR, CcpN, FruR) are regulated by yet unknown effectors. Overall, both nutrient shifts induced substantial, global network reconfiguration at all levels of regulation.

To identify the relevant primary changes in central metabolism, where essentially all genes were differentially expressed during one or both shifts, we correlated time courses of metabolic fluxes with those of the abundances of the corresponding enzymes. We estimated dynamic extracellular rates by interpolation (SOM 3) and network-wide pseudodynamic metabolic fluxes with a stoichiometric network model and the intracellular metabolite concentrations (Fig. 3, B and C, and SOM 4). Positive correlations between fluxes and enzyme abundances indicated genetic rather than metabolic regulation of the reaction rates (*21*). Upon the addition of malate, the abundances of only the nicotinamide adenine dinucleotide phosphate–dependent malic enzyme (YtsJ) and two acetate production enzymes (Pta and AckA) correlated with their respective reaction rates ($R > 0.8$) and thus putatively control flux (Fig. 4A). After the addition of glucose, enzymes for 11 central reactions putatively controlled flux, and in six cases increasing enzyme abundance potentially overcame the bottleneck in glucose uptake. The corresponding genes are organized in two operons: *ptsGHI* for glucose transport and phosphorylation and *cggR-gapA-pgk-tpiA-pgm-eno* for lower glycolysis. This focused analysis of multiple "omics" data sets suggested the *pts* and *cggR* operons as primary control targets for adaptation, where the half-maximal responses of the *pts* and *cggR* operon-encoded proteins within 30 to 60 min of glucose addition could account for the ~60-min delay in glucose uptake (Fig. 2, B and C). We evaluated the relative contributions of both operons to the delay with a *cggR* deletion mutant and a mutant with constitutive *ptsG* expression (Fig. 4B and SOM 5). When grown on malate, both mutants used glucose immediately without the delay of the wild-type strain. As the *cggR* or *ptsG* expression alone is sufficient to facilitate immediate glucose uptake, it is not obvious why *B. subtilis* does not express these genes constitutively.

B. subtilis needs to optimize its use of two qualitatively distinct substrates: Glucose results in high growth yields at low metabolic rates, whereas malate results in low growth yields at high metabolic rates (*13*). Similar trade-offs exist between respiratory and fermentative strategies in adenosine triphosphate generation, both of which can confer condition-specific evolutionary advantages (*22*). To investigate optimal control strategies for substrate usage in *Bacillus*, we developed a simplified dynamic model that describes the substrate and biomass dynamics of the shift experiments quantitatively (SOM 6). The maintenance cost for enzyme expression (ρ) is a key parameter in the model; the estimated value of $\rho_0 \approx 0.06$ implies that full expression of a metabolic (substrate) system would reduce the maximal specific growth rate by ≈5%. In silico

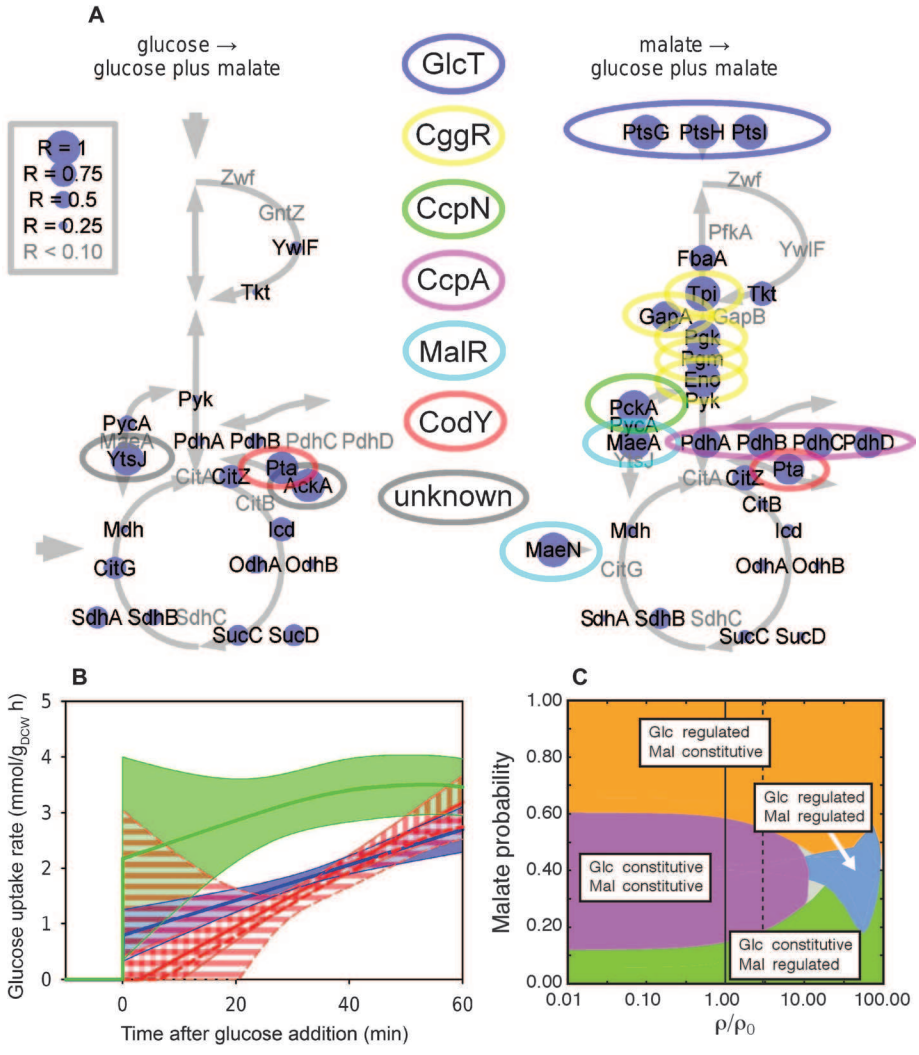

Fig. 4. (**A**) Regulatory mechanisms relevant for control of metabolic fluxes during the two shifts. Key controlling enzymes are indicated by a positive correlation between reaction rate and enzyme abundance after addition of malate (left) or glucose (right). Reactions were considered only if both enzyme abundance and flux changed by more than one standard deviation and if the correlation coefficient was positive. The size of the purple circles is proportional to the correlation coefficient (see inset). Transcription factors (middle) were identified by network component analysis to be responsible for changes in enzyme expression, as indicated by color coding (gray denotes unknown factors). (**B**) Dynamics of glucose uptake rate upon addition of glucose to a culture growing exponentially on malate in mutants with constitutive *ptsG* expression (green), *cggR* deletion (blue), and the respective parent strains (solid red, vertical shading and dashed red, horizontal shading). Shaded areas denote 95% pointwise confidence intervals. g_{DCW}, grams of dry cell weight. (**C**) Predicted growth effects of different control strategies using a simplified dynamic model. In silico competition experiments were carried out between two strains that differ in how they control malate and glucose uptake; both systems can be expressed constitutively or only upon substrate availability (SOM 6). Cocultures in a chemostat setting were pulsed every 3 hours with substrate (similar results were obtained with pulse frequencies of 1 and 9 hours), where the probability of selecting malate versus glucose as substrate was varied. The cost of metabolic system maintenance (ρ) normalized by the estimated cost for *B. subtilis* (ρ_0; the solid line indicates the estimated value of ρ; the dashed line to the right is the upper bound of the 95% confidence interval) constituted a free simulation parameter. Control strategies with higher growth rates were considered advantageous, and the best control strategies are identified by color coding.

competition of strains that either constitutively express the metabolic systems or induce their expression only upon substrate availability allowed us to quantify the dynamic control effects. In simulations of a dynamically changing environment, we varied the substrate probabilities and the maintenance cost ρ because of the uncertainties in the estimated ρ_0 (Fig. 4C). Surprisingly, there almost always existed a unique, evolutionarily dominating control strategy. The winning strategy depended on quantitative parameters. Hence, active regulation or constitutive subsystem expression are not advantageous per se. Even with the uncertainties in ρ_0, the experimentally observed strategy of constitutive malate usage capacity (Fig. 2B) but induced (and delayed) glucose-specific metabolism confers an evolutionary advantage if *B. subtilis* predominantly encounters malate (Fig. 4C). This is biologically plausible given the organism's habitat in the vicinity of plant root systems that often secrete carboxylic acids such as malate (*13*, *23*).

Our systems approach helps reveal how previously known regulatory mechanisms are combined to effect nutritional transitions. Despite more than half of the *B. subtilis* gene complement being involved in the adaptive response to glucose, our methodology could discern the key regulatory events. The overall control strategy of *B. subtilis* can be rationalized in terms of its evolutionary advantages; however, these advantages, and therefore the overall control design, depend on quantitative system characteristics—regulation is not beneficial per se. The dynamic data presented here may be used for further computational analyses such as multivariate statistics and large-scale structural or kinetic network models (*24*). We hope that our publicly available tools for mathematical analyses and modeling will facilitate future large-scale and dynamic systems biology studies in *B. subtilis* and other species.

References and Notes

1. U. Sauer, M. Heinemann, N. Zamboni, *Science* **316**, 550 (2007).
2. M. Ralser *et al.*, *Nat. Biotechnol.* **27**, 604 (2009).
3. G. Chechik *et al.*, *Nat. Biotechnol.* **26**, 1251 (2008).
4. N. Ishii *et al.*, *Science* **316**, 593 (2007).
5. E. Yus *et al.*, *Science* **326**, 1263 (2009).
6. M. Güell *et al.*, *Science* **326**, 1268 (2009).
7. J. F. Moxley *et al.*, *Proc. Natl. Acad. Sci. U.S.A.* **106**, 6477 (2009).
8. A. B. Canelas *et al.*, *Nat. Comm.* **1**, 145 (2010).
9. M. T. A. P. Kresnowati *et al.*, *Mol. Syst. Biol.* **2**, 49 (2006).
10. M. J. Brauer *et al.*, *Proc. Natl. Acad. Sci. U.S.A.* **103**, 19302 (2006).
11. S. Jozefczuk *et al.*, *Mol. Syst. Biol.* **6**, 364 (2010).
12. P. H. Bradley, M. J. Brauer, J. D. Rabinowitz, O. G. Troyanskaya, *PLOS Comput. Biol.* **5**, e1000270 (2009).
13. R. J. Kleijn *et al.*, *J. Biol. Chem.* **285**, 1587 (2010).
14. E. Botella *et al.*, *Microbiology* **156**, 1600 (2010).
15. Materials and methods are available as supporting material on *Science* Online.
16. S. Haykin, *Kalman Filtering and Neural Networks* (Wiley-Interscience, New York, 2001).
17. A. L. Sonenshein, *Nat. Rev. Microbiol.* **5**, 917 (2007).
18. T. Doan, S. Aymerich, *Mol. Microbiol.* **47**, 1709 (2003).
19. A. Goelzer *et al.*, *BMC Syst. Biol.* **2**, 20 (2008).
20. J. C. Liao *et al.*, *Proc. Natl. Acad. Sci. U.S.A.* **100**, 15522 (2003).
21. S. Rossell *et al.*, *Proc. Natl. Acad. Sci. U.S.A.* **103**, 2166 (2006).
22. T. Pfeiffer, S. Schuster, S. Bonhoeffer, *Science* **292**, 504 (2001).
23. H. P. Bais, T. L. Weir, L. G. Perry, S. Gilroy, J. M. Vivanco, *Annu. Rev. Plant Biol.* **57**, 233 (2006).
24. M. Heinemann, U. Sauer, *Curr. Opin. Microbiol.* **13**, 337 (2010).

Acknowledgments: This work was funded through the European Commission 7th Framework project BaSysBio (LSHG-CT-2006-037469), coordinated by P. Noirot, the Department of Education, Science and Training (CG110055), and the National Health and Medical Research Council (455646). Data, algorithms, and mathematical models have been deposited in a publicly accessible relational database (www.basysbio.eu/nutrientshift/ and table S1).

Supporting Online Material

www.sciencemag.org/cgi/content/full/335/6072/1099/DC1
Materials and Methods
SOM Text (SOM 1 to 6)
Figs. S1 to S20
Tables S1 to S8
References (*25*–*28*)
Database S1

12 April 2011; accepted 11 January 2012
10.1126/science.1206871

Condition-Dependent Transcriptome Reveals High-Level Regulatory Architecture in *Bacillus subtilis*

Pierre Nicolas,[1]* Ulrike Mäder,[2,3]* Etienne Dervyn,[4]* Tatiana Rochat,[4] Aurélie Leduc,[1] Nathalie Pigeonneau,[4] Elena Bidnenko,[4] Elodie Marchadier,[4] Mark Hoebeke,[1] Stéphane Aymerich,[4] Dörte Becher,[2] Paola Bisicchia,[5] Eric Botella,[5] Olivier Delumeau,[4] Geoff Doherty,[6] Emma L. Denham,[7] Mark J. Fogg,[8] Vincent Fromion,[1] Anne Goelzer,[1] Annette Hansen,[5] Elisabeth Härtig,[9] Colin R. Harwood,[10] Georg Homuth,[3] Hanne Jarmer,[11] Matthieu Jules,[4] Edda Klipp,[12] Ludovic Le Chat,[4] François Lecointe,[4] Peter Lewis,[6] Wolfram Liebermeister,[12] Anika March,[9] Ruben A. T. Mars,[7] Priyanka Nannapaneni,[3] David Noone,[5] Susanne Pohl,[10] Bernd Rinn,[13] Frank Rügheimer,[14] Praveen K. Sappa,[3] Franck Samson,[1] Marc Schaffer,[2] Benno Schwikowski,[14] Leif Steil,[3] Jörg Stülke,[15] Thomas Wiegert,[16] Kevin M. Devine,[5] Anthony J. Wilkinson,[8] Jan Maarten van Dijl,[7] Michael Hecker,[2] Uwe Völker,[3] Philippe Bessières,[1] Philippe Noirot[4]†

Bacteria adapt to environmental stimuli by adjusting their transcriptomes in a complex manner, the full potential of which has yet to be established for any individual bacterial species. Here, we report the transcriptomes of *Bacillus subtilis* exposed to a wide range of environmental and nutritional conditions that the organism might encounter in nature. We comprehensively mapped transcription units (TUs) and grouped 2935 promoters into regulons controlled by various RNA polymerase sigma factors, accounting for ~66% of the observed variance in transcriptional activity. This global classification of promoters and detailed description of TUs revealed that a large proportion of the detected antisense RNAs arose from potentially spurious transcription initiation by alternative sigma factors and from imperfect control of transcription termination.

Bacterial transcriptomes are surprisingly complex (*1*–*5*) and include diverse and abundant small RNAs and antisense RNAs (asRNAs). Because only a small number of environmental conditions have been investigated, the full extent of transcriptome complexity remains to be established for a single bacterial species. This prompted us to undertake a systematic and quantitative exploration of transcriptome changes in *Bacillus subtilis*, whose natural habitat, the soil, is subject to severe environmental fluctuations (*6*). *B. subtilis* is also a laboratory model for Gram-positive bacteria and is grown in industrial-scale fermentors for the production of enzymes and vitamins. We selected 104 conditions covering

[1]INRA, UR1077, Mathématique Informatique et Génome, F-78350 Jouy-en-Josas, France. [2]Institute for Microbiology, Ernst-Moritz-Arndt University Greifswald, D-17489 Greifswald, Germany. [3]Interfaculty Institute for Genetics and Functional Genomics, Ernst-Moritz-Arndt-University Greifswald, D-17489 Greifswald, Germany. [4]INRA, UMR1319 Micalis, F-78350 Jouy-en-Josas, France. [5]Smurfit Institute of Genetics, Trinity College Dublin, Dublin 2, Ireland. [6]School of Environmental and Life Sciences, University of Newcastle, Callaghan, NSW 2308, Australia. [7]Department of Medical Microbiology, University of Groningen and University Medical Center Groningen, 9700 RB Groningen, Netherlands. [8]York Structural Biology Laboratory, Department of Chemistry, University of York, York YO10 5YW, UK. [9]Institute of Microbiology, Technical University of Braunschweig, D-38106 Braunschweig, Germany. [10]Centre for Bacterial Cell Biology, Institute, of Cell and Molecular Biosciences, Newcastle University of Newcastle, Newcastle upon Tyne, NE2 4AX, UK. [11]Center for Biological Sequence Analysis, Department of Systems Biology, Technical University of Denmark, 2800 Kgs. Lyngby, Denmark. [12]Theoretical Biophysics, Humboldt University Berlin, 10115 Berlin, Germany. [13]Center for Information Sciences and Databases, Department of Biosystems Science and Engineering, ETH Zurich, 4058 Basel, Switzerland. [14]Systems Biology Lab and CNRS URA 2171, Institut Pasteur, 75724 Paris cedex 15, France. [15]Department of General Microbiology, Georg-August-University Göttingen, D-37077 Göttingen, Germany. [16]FN Biotechnologie, Hochschule Zittau/Görlitz, D-02763 Zittau, Germany.

*These authors contributed equally to this work.
†To whom correspondence should be addressed. E-mail: philippe.noirot@jouy.inra.fr